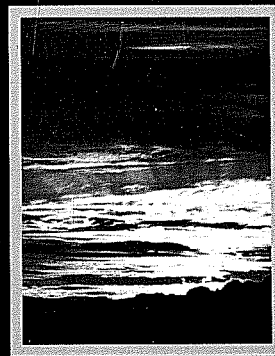
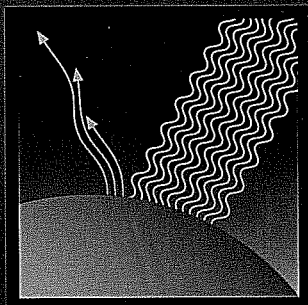


# An Introduction to Atmospheric Radiation

SECOND  
EDITION



K. N. LIOU



INTERNATIONAL GEOPHYSICS SERIES, VOLUME 84



in Section 4.5. Exercise 3.6 requires the evaluation of spectral absorptance in the limit of strong line approximation using the Lorentz line shape. The total amount of water vapor can be estimated by this approximation using the  $0.94 \mu\text{m}$  band, which is the foundation for the determination of precipitable water from sunphotometers (see Section 7.2).

Figure 3.9 shows the depletion of solar flux in a clear atmosphere. The top curve is an observed solar irradiance with a spectral resolution of  $50 \text{ cm}^{-1}$  at the top of the earth's atmosphere as depicted in Fig 2.9. The depletion of solar irradiance in the UV region ( $<0.4 \mu\text{m}$ ) is chiefly due to the absorption of molecular oxygen and ozone discussed previously. In the visible, the depletion of solar flux is caused by the absorption produced by oxygen red bands, the ozone Chappuis band, and some water vapor weak bands; but the chief attenuation is associated with Rayleigh scattering to be discussed in Section 3.3. In the near-IR, the prime absorber is water vapor with contributions from carbon dioxide in the  $2.7 \mu\text{m}$  band. Other minor absorbers such as  $\text{N}_2\text{O}$ ,  $\text{CO}$ , and  $\text{CH}_4$  also contribute to the depletion of solar flux but are less significant. It is evident that water vapor is the most important absorber in the solar near-IR spectrum, which contains about 50% of solar energy.

### 3.3 Atmospheric Scattering

#### 3.3.1 Rayleigh Scattering

The simplest and in some ways the most important example of a physical law of light scattering with various applications is that discovered by Rayleigh (1871). His findings led to the explanation of the blue color of the sky. In this section we formulate the scattering of unpolarized sunlight by air molecules and describe its important application to the atmosphere.

##### 3.3.1.1 THEORETICAL DEVELOPMENT

Consider a small homogeneous, isotropic, spherical particle whose radius is much smaller than the wavelength of the incident radiation. The incident radiation produces a homogeneous electric field  $\mathbf{E}_0$ , called the *applied field*. Since the particle is very small, the applied field generates a dipole configuration on it. The electric field of the particle, caused by the electric dipole, modifies the applied field inside and near the particle. Let  $\mathbf{E}$  be the combined field, i.e., the applied field plus the particle's own field, and further, let  $\mathbf{p}_0$  be the induced dipole moment. Then we apply the electrostatic formula to give

$$\mathbf{p}_0 = \alpha \mathbf{E}_0. \quad (3.3.1)$$

This equation defines the polarizability  $\alpha$  of a small particle. The dimensions of  $\mathbf{E}_0$  and  $\mathbf{p}_0$  are in units of charge per area and charge times length, respectively, and  $\alpha$  has the dimension of volume. In general,  $\alpha$  is a tensor, because the vectors  $\mathbf{p}_0$  and  $\mathbf{E}_0$  may not align along the three mutually perpendicular directions. In the very common case where these two vectors coincide,  $\alpha$  is a scalar.

The applied field  $\mathbf{E}_0$  generates oscillation of an electric dipole in a fixed direction. The oscillating dipole, in turn, produces a plane-polarized electromagnetic wave, the scattered wave. To evaluate the scattered electric field in regions that are far away from the dipole, we let  $r$  denote the distance between the dipole and the observation point,  $\gamma$  the angle between the scattered dipole moment  $\mathbf{p}$  and the direction of observation, and  $c$  the velocity of light. According to the classical electromagnetic solution given by Hertz (1889), the scattered electric field is proportional to the acceleration of the scattered dipole moment and  $\sin \gamma$ , but is inversely proportional to the distance  $r$ . Thus, we have

$$\mathbf{E} = \frac{1}{c^2} \frac{1}{r} \frac{\partial^2 \mathbf{p}}{\partial t^2} \sin \gamma. \quad (3.3.2)$$

In an oscillating periodic field, the scattered dipole moment may be written in terms of the induced dipole moment as

$$\mathbf{p} = \mathbf{p}_0 e^{-ik(r-ct)}. \quad (3.3.3)$$

Note that  $k$  is the wavenumber, and  $kc = \omega$  is the circular frequency. By combining Eqs. (3.3.1) and (3.3.3), Eq. (3.3.2) yields

$$\mathbf{E} \propto \frac{1}{\lambda^2} \quad \mathbf{E} = -\mathbf{E}_0 \frac{e^{-ik(r-ct)}}{r} k^2 \alpha \sin \gamma. \quad k^2 = \frac{\omega^2}{c^2} \quad (3.3.4)$$

Now we consider the scattering of sunlight by air molecules. Let the plane defined by the directions of incident and scattered waves be the reference plane (plane of scattering). Since any electric vector may be arbitrarily decomposed into orthogonal components, we may choose the two components perpendicular ( $E_r$ ) and parallel ( $E_l$ ) to the plane of scattering. The sunlight is characterized by the same electric field in the  $r$  and  $l$  directions and by a random phase relation between these two components, and is referred to as *natural* or *unpolarized* light (see Section 6.6 for a more advanced discussion of the representation of polarized light). In this case, we may consider separately the scattering of the two electric field components  $E_{0r}$  and  $E_{0l}$  by molecules assumed to be homogeneous, isotropic, spherical particles. Based on Eq. (3.3.4), we have

$$E_r = -E_{0r} \frac{e^{-ik(r-ct)}}{r} k^2 \alpha \sin \gamma_1, \quad (3.3.5a)$$

$$E_l = -E_{0l} \frac{e^{-ik(r-ct)}}{r} k^2 \alpha \sin \gamma_2. \quad (3.3.5b)$$

Referring to Fig. 3.10, we see that  $\gamma_1 = \pi/2$  and  $\gamma_2 = \pi/2 - \Theta$ , where  $\Theta$  is defined as the scattering angle, which is the angle between the incident and scattered waves. Note that  $\gamma_1$  is always equal to  $90^\circ$  because the scattered dipole moment (or the scattered electric field) in the  $r$  direction is normal to the scattering plane defined previously.

In matrix form, we may write

$$\begin{bmatrix} E_r \\ E_l \end{bmatrix} = -\frac{e^{-ik(r-ct)}}{r} k^2 \alpha \begin{bmatrix} 1 & 0 \\ 0 & \cos \Theta \end{bmatrix} \begin{bmatrix} E_{0r} \\ E_{0l} \end{bmatrix}. \quad (3.3.6)$$

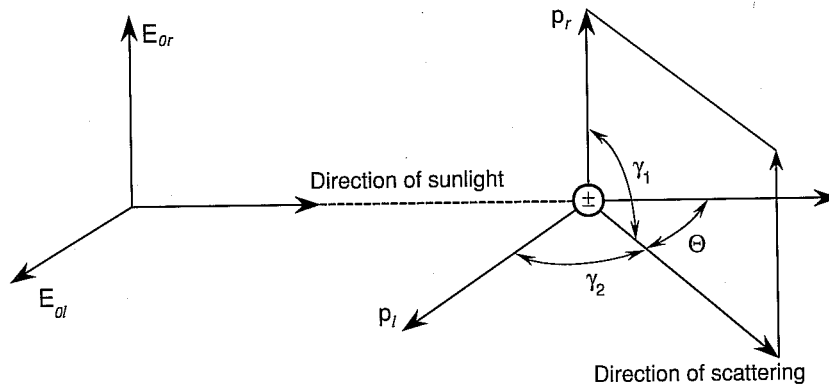


**Figure 3.10** Scattering by a dipole. The incident electric field, a vector, can be arbitrarily decomposed into a parallel ( $l$ ) and a perpendicular ( $r$ ) component, where each undergoes the scattering by the dipole. We may select the component that is always perpendicular to the scattering plane that is defined by the incident and scattering beams (i.e.,  $\gamma_1 = 90^\circ$ ). All the notations are defined in the text.

A complete description of the intensity of a light beam and its polarized state will be given in Section 6.6 in which the Stokes parameters are introduced. For the sake of the continuity of the present discussion, however, we may define the intensity components (per solid angle) of the incident and scattered radiation in the forms  $I_0 = C|E_0|^2$  and  $I = C|E|^2$ , where  $C$  is a certain proportionality factor such that  $C/r^2$  implies a solid angle. It follows that Eqs. (3.3.5) and (3.3.6) can be expressed in the form of intensities as

$$I_r = I_0 k^4 \alpha^2 / r^2, \quad (3.3.7a)$$

$$I_l = I_0 k^4 \alpha^2 \cos^2 \Theta / r^2, \quad (3.3.7b)$$

where  $I_r$  and  $I_l$  are polarized intensity components perpendicular and parallel to the plane containing the incident and scattered waves, i.e., the plane of scattering. The total scattered intensity of the unpolarized sunlight incident on a molecule in the direction of  $\Theta$  is then

$$I = I_r + I_l = (I_{0r} + I_{0l} \cos^2 \Theta) k^4 \alpha^2 / r^2. \quad (3.3.8)$$

But for unpolarized sunlight,  $I_{0r} = I_{0l} = I_0/2$ , and by noting that  $k = 2\pi/\lambda$ , we obtain

$$I = \frac{I_0}{r^2} \alpha^2 \left( \frac{2\pi}{\lambda} \right)^4 \frac{1 + \cos^2 \Theta}{2}. \quad (3.3.9)$$

This is the original formula derived by Rayleigh, and we call the scattering of sunlight by molecules Rayleigh scattering. By this formula, the intensity of unpolarized sunlight scattered by a molecule is proportional to the incident intensity  $I_0$  and is inversely proportional to the square of the distance between the molecule and the

point of observation. In addition to these two factors, the scattered intensity also depends on the polarizability, the wavelength of the incident wave, and the scattering angle. The dependence of these three parameters on the scattering of sunlight by molecules introduces a number of significant physical features.

### 3.3.1.2 PHASE FUNCTION, SCATTERING CROSS SECTION, AND POLARIZABILITY

On the basis of Eqs. (3.3.7) and (3.3.9), the intensity scattered by a molecule depends on the polarization characteristics of the incident light. For vertically ( $r$ ) polarized incident light, the scattered intensity is independent of the direction of the scattering plane. In this case then, the scattering is isotropic. On the other hand, for horizontally ( $l$ ) polarized incident light, the scattered intensity is a function of  $\cos^2 \Theta$ . When the incident light is unpolarized, such as sunlight, the scattered intensity depends on  $(1 + \cos^2 \Theta)$ . The angular scattering patterns in space for the three types of incident polarization are illustrated in Fig. 3.11. We see that the scattering of unpolarized sunlight by molecules (Rayleigh scattering) has maxima in the forward ( $0^\circ$ ) and backward ( $180^\circ$ ) directions, whereas it shows minima in the side directions ( $90^\circ$  and  $270^\circ$ ). Light scattered by particles or molecules is not confined only to the plane of incidence, but is visible in all azimuthal directions. Because of the spherical symmetry assumed for molecules, scattering patterns are symmetrical in three-dimensional space, as demonstrated in Fig. 3.11.

To describe the angular distribution of scattered energy in conjunction with multiple scattering and radiative transfer analyses and applications for planetary atmospheres, we find it necessary to define a nondimensional parameter called the *phase function*,  $P(\cos \Theta)$ , such that

$$\int_0^{2\pi} \int_0^\pi \frac{P(\cos \Theta)}{4\pi} \sin \Theta d\Theta d\phi = 1. \quad (3.3.10)$$

By this definition, the phase function is said to be normalized to unity. Upon performing simple integrations, the phase function of Rayleigh scattering for incident unpolarized sunlight is given by

$$P(\cos \Theta) = \frac{3}{4}(1 + \cos^2 \Theta). \quad (3.3.11)$$

Employing the definition of the phase function, Eq. (3.3.9) may be rewritten in the form

$$I(\Theta) = \frac{I_0}{r^2} \alpha^2 \frac{128\pi^5}{3\lambda^4} \frac{P(\Theta)}{4\pi}. \quad (3.3.12)$$

It follows that the angular distribution of the scattered intensity is directly proportional to the phase function.

The scattered flux  $f$  (or power, in units of energy per time) can be evaluated by integrating the scattered flux density ( $I \Delta \Omega$ ) over the appropriate area a distance  $r$

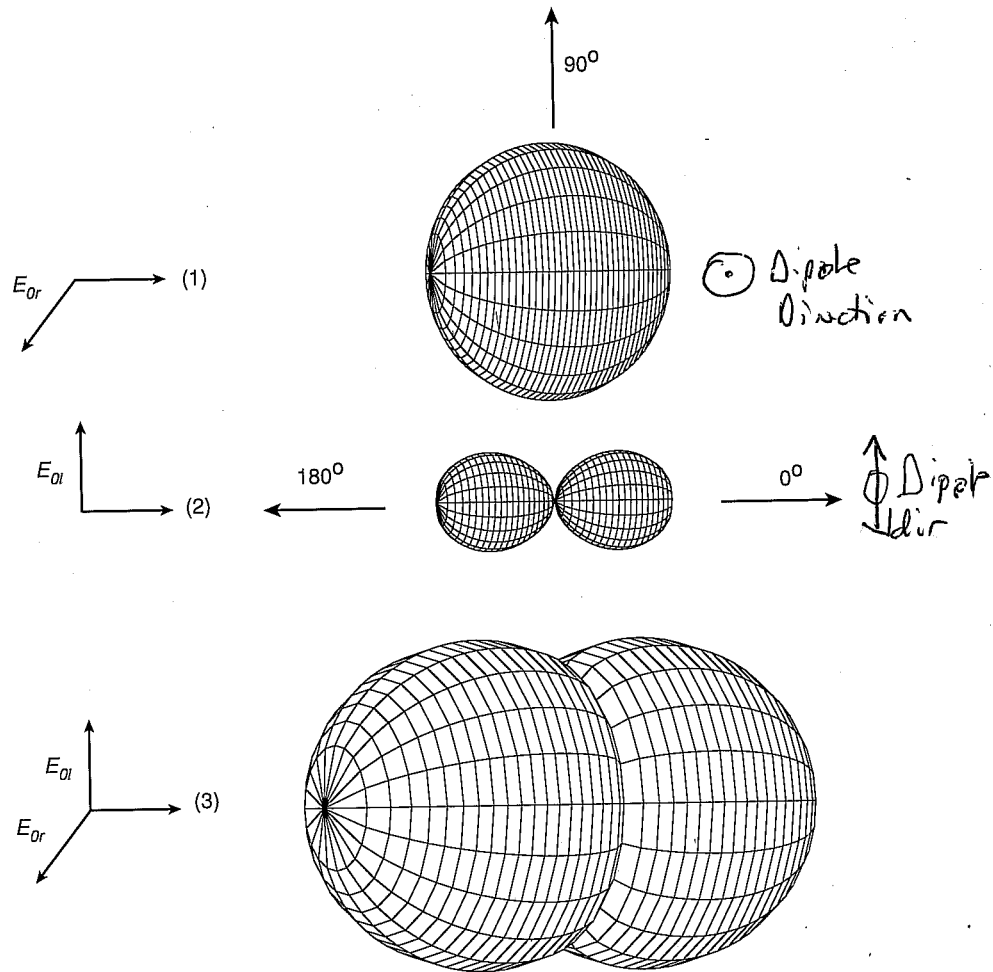


**Figure 3.11** Polar diagram of the scattered intensity for Rayleigh molecules: (1) polarized incident light with the electric vector perpendicular to the scattering plane, (2) polarized incident light with the electric vector on the scattering plane, and (3) unpolarized incident light.

away from the scatterer. Thus,

$$f = \int_{\Omega} (I \Delta \Omega) r^2 d\Omega, \tag{3.3.13a}$$

where  $r^2 d\Omega$  represents the area according to the definition of the solid angle. Inserting the expressions for scattered intensity and the differential solid angle defined in Eqs. (3.3.12) and (1.1.5), respectively, into Eq. (3.3.13a) and carrying out integrations over the solid angle of a sphere, we obtain the equivalent isotropically scattered flux

in the form

$$f = F_0 \alpha^2 128 \pi^5 / (3 \lambda^4), \quad (3.3.13b)$$

where the incident flux density  $F_0$  is equal to  $I_0 \Delta \Omega$ . Moreover, we may define the scattering cross section per one molecule as

$$\sigma_s = f / F_0 = \alpha^2 128 \pi^5 / (3 \lambda^4). \quad (3.3.14)$$

The scattering cross section (in units of area) represents the amount of incident energy that is removed from the original direction because of a single scattering event such that the energy is redistributed isotropically on the area of a sphere whose center is the scatterer and whose radius is  $r$ . In terms of the scattering cross section, the scattered intensity can be expressed by

$$I(\Theta) = I_0 \frac{\sigma_s}{r^2} \frac{P(\Theta)}{4\pi}. \quad (3.3.15)$$

This is the general expression for scattered intensity, which is valid not only for molecules but also for particles whose size is larger than the incident wavelength, as will be discussed in Section 5.2.

The polarizability  $\alpha$ , which was used in the preceding equations, can be derived from the principle of the dispersion of electromagnetic waves and is given by

$$\alpha = \frac{3}{4\pi N_s} \left( \frac{m^2 - 1}{m^2 + 2} \right), \quad N_s = \frac{\rho_s}{\text{mol weight} \times N_A} \quad N_s = 1/\text{volume for molecule} \quad (3.3.16)$$

where  $N_s$  is the total number of molecules per unit volume and  $m$  is the nondimensional refractive index of molecules. This equation is called the *Lorentz-Lorenz formula*, and its derivation is given in Appendix D. The refractive index is an optical parameter associated with the velocity change of electromagnetic waves in a medium with respect to a vacuum. Its definition and physical meanings are also given in Appendix D. Normally, the refractive indices of atmospheric particles and molecules are composed of a real part  $m_r$  and an imaginary part  $m_i$ , corresponding, respectively, to the scattering and absorption properties of particles and molecules. In the solar visible spectrum, the imaginary parts of the refractive indices of air molecules are so insignificantly small that absorption of solar radiation by air molecules may be neglected in the scattering discussion. The real parts of the refractive indices of air molecules in the solar spectrum are very close to 1, but they depend on the wavelength (or frequency) of the incident radiation as illustrated in Appendix D. Because of this dependence, white light may be *dispersed* into component colors by molecules that function like prisms. The real part of the refractive index derived in Appendix D [(Eq. D.17)] may be approximately fitted by

$$(m_r - 1) \times 10^8 = 6432.8 + \frac{2,949,810}{146 - \lambda^{-2}} + \frac{25,540}{41 - \lambda^{-2}},$$

Refractive index for Air  
(Real Part)

$\lambda$  in  $\mu\text{m}$   
(3.3.17)

See  
Level

where  $\lambda$  is in units of micrometers. Since  $m_r$  is close to 1, for all practical purposes, Eq. (3.3.16) may be approximated by

$$\alpha \approx \frac{1}{4\pi N_s} (m_r^2 - 1). \tag{3.3.18}$$

Thus, the scattering cross section defined in Eq. (3.3.14) becomes

*per molecule*  
 $N_s \sim 2.69 \times 10^{19}/cc$

$$\sigma_s = \frac{8\pi^3 (m_r^2 - 1)^2}{3\lambda^4 N_s^2} f(\delta). \tag{3.3.19}$$

*$N_s = \frac{\# \text{ molecules}}{\text{volume}}$   
 @ Sea Level*

A correction factor  $f(\delta)$  is added in Eq. (3.3.19) to take into consideration the anisotropic property of molecules, where  $f(\delta) = (6 + 3\delta)/(6 - 7\delta)$  with the anisotropic factor  $\delta$  of 0.035. Anisotropy implies that the refractive index of molecules varies along the  $x$ ,  $y$ , and  $z$  directions, and thus is a vector, not a scalar. Hence, the polarizability  $\alpha$  is a tensor, as noted previously. *for air? likely.  $f(\delta) = 1.06$*

The optical depth of the entire molecular atmosphere at a given wavelength may be calculated from the scattering cross section in the form

$$\tau(\lambda) = \sigma_s(\lambda) \int_0^{z_\infty} N(z) dz, \tag{3.3.20}$$

where  $N(z)$  denotes the number density of molecules as a function of height, and  $z_\infty$  is the top of the atmosphere. The optical depth represents the attenuation power of molecules with respect to a specific wavelength of the incident light. Exercises 3.7–3.11 require the calculation of a number of parameters based on Rayleigh scattering results.

### 3.3.1.3 BLUE SKY AND SKY POLARIZATION

Returning to Eq. (3.3.12), we see that the scattered intensity depends on the wavelength of incident light and the index of refraction of air molecules contained in the polarizability term. According to the analyses given in Appendix D and Eq. (3.3.17), the index of refraction also depends slightly on the wavelength. However, the dependence of the refractive index on the wavelength is relatively insignificant in calculating the scattered intensity as compared to the explicit wavelength term. Thus, the intensity scattered by air molecules in a specific direction may be symbolically expressed in the form

$$I_\lambda \sim 1/\lambda^4. \tag{3.3.21}$$

The inverse dependence of the scattered intensity on the wavelength to the fourth power is a direct consequence of the theory of Rayleigh scattering and is the foundation for the explanation of blue sky.

In reference to the observed solar energy spectrum displayed in Fig. 3.9, a large portion of solar energy is contained between the blue and red regions of the visible spectrum. Blue light ( $\lambda \approx 0.425 \mu\text{m}$ ) has a shorter wavelength than red light ( $\lambda \approx 0.650 \mu\text{m}$ ). Consequently, according to Eq. (3.3.21) blue light scatters about 5.5 times

more intensity than red light. It is apparent that the  $\lambda^{-4}$  law causes more blue light to be scattered than red, green, and yellow, and so the sky, when viewed away from the sun's disk, appears blue. Moreover, since molecular density decreases drastically with height, it is anticipated that the sky should gradually darken to become completely black in outer space in directions away from the sun. And the sun itself should appear whiter and brighter with increasing height. As the sun approaches the horizon (at sunset or sunrise), sunlight travels through more air molecules, and therefore more and more blue light and light with shorter wavelengths are scattered out of the beam of light, and the luminous sun shows a deeper red color than at its zenith. However, since violet light ( $\sim 0.405 \mu\text{m}$ ) has a shorter wavelength than blue, a reasonable question is, why doesn't the sky appear violet? This is because the energy contained in the violet spectrum is much less than that contained in the blue spectrum, and also because the human eye has a much lower response to the violet color.

Another important phenomenon explained by the Rayleigh scattering theory is sky polarization. For many atmospheric remote sensing applications utilizing polarization, a parameter called the *degree of linear polarization* has been used (Subsection 7.3.5.2). In the case of Rayleigh scattering it is given by

$$LP(\Theta) = -\frac{I_l - I_r}{I_l + I_r} = -\frac{\cos^2 \Theta - 1}{\cos^2 \Theta + 1} = \frac{\sin^2 \Theta}{\cos^2 \Theta + 1}. \quad (3.3.22)$$

In the forward and backward directions the scattered light remains completely unpolarized, whereas at the  $90^\circ$  scattering angle, the scattered light becomes completely polarized. In other directions, the scattered light is partially polarized with the percentage of polarization ranging from 0 to 100%. Interested readers may wish to refer to Section 6.6 for further details on this subject.

The theory of Rayleigh scattering developed in Section 3.3.1 is based on the assumption that molecules are homogeneous and isotropic spheres. However, molecules are in general anisotropic, whereby their polarizability, as defined in Eq. (3.3.16), varies along three axes and, hence, is a tensor instead of a scalar. The anisotropic effect of molecules reduces the degree of linear polarization defined in Eq. (3.3.22) by only a small percentage. At the  $90^\circ$  scattering angle, the degree of linear polarization for dry air is about 0.94. Further, the theory of Rayleigh scattering developed previously considers only single (or primary) scattering, i.e., where scattering occurs only once. But in the earth's atmosphere, which contains a large number of molecules and aerosol particles, light may undergo an infinite number of scattering events. In addition, the earth's surface also reflects light that reaches it. Multiple scattering processes involving the atmosphere and the surface become complicated and require a more advanced treatment of radiative transfer theory, which will be discussed in Chapter 6.

The theory of Rayleigh scattering predicts *neutral points*, i.e., points of zero polarization, only at the exact forward and backward directions. However, owing to multiple scattering of molecules and particulates, and reflection of the surface, there normally exist a number of neutral points in cloudless atmospheres. The first observations of neutral points and partially polarized sky light were made by Arago in

1809. He discovered the existence of a neutral point at a position in the sky about  $25^\circ$  above the antisolar direction (the direction exactly opposite that of the sun). The other two neutral points, which normally occur in the sunlit sky  $25^\circ$  above and  $20^\circ$  below the sun, were discovered by Babinet in 1840 and by Brewster in 1842, respectively. These three neutral points were named to honor these three discoverers. The neutral points in the sky vary and depend on the turbidity (an indication of the amount of aerosol loadings in the atmosphere), the sun's elevation angle, and the reflection characteristics of the surface at which observations are made.

Figure 3.12 illustrates the distribution of the degree of polarization and neutral points for a pristine, clear atmosphere (January 20, 1977) and for an atmospheric condition under the El Chichon volcanic cloud (July 27, 1982) observed at the Mauna Loa Observatory from a polarimeter developed by Coulson (1983). The observations

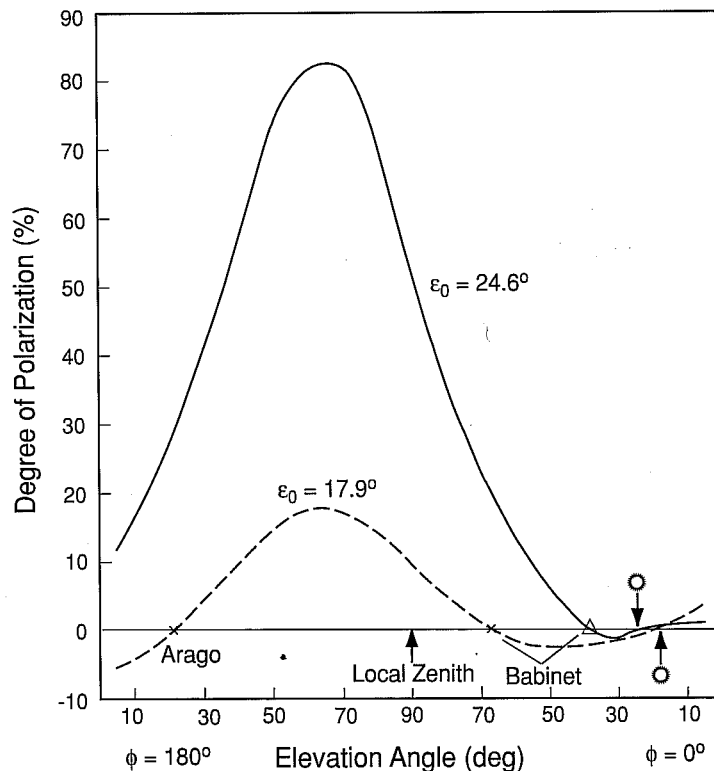


**Figure 3.12** Illustration of neutral points in the distribution of the degree of polarization through the plane of the sun's vertical at a wavelength of  $0.7 \mu\text{m}$  observed at the Mauna Loa Observatory for a clear atmospheric condition on January 20, 1977 (solid line), and for an atmosphere under the volcanic cloud on July 27, 1982 (dashed line). The azimuthal angles  $\phi = 0^\circ$  and  $\phi = 180^\circ$  are on the sun's vertical plane. The sun's elevation angles  $\epsilon_0$  for these two cases are indicated in the graph, as are the positions of Arago and Babinet (data taken from Coulson, 1983).

were made on the sun's vertical plane, referred to as the principal plane in radiative transfer, using a wavelength of  $0.7 \mu\text{m}$ . The solar elevation angle,  $\varepsilon_0$  ( $90^\circ -$  solar zenith angle  $\theta_0$ ), differed slightly on these two dates, but the observed polarization patterns suffice to demonstrate their substantial variabilities in clear and turbid atmospheres. The clear Rayleigh atmosphere produced a maximum polarization of about 80%, 60% more than that generated in the volcanic cloud condition. The neutral points in the Rayleigh scattering atmosphere occurred at the positions close to the sun (forward direction) and about  $20^\circ$  above the sun, the Babinet point, which was about  $50^\circ$  above the sun when a significant aerosol loading was present. In this case, the Arago point was also shown at about  $20^\circ$  above the horizon at the opposite position of the sun. Because of the sun's position, the Brewster point was not observed. The neutral points' positions are dependent on the aerosol optical depth and composition. Thus, a systematic observation of these points could be a valuable approach for inferring aerosol optical properties and perhaps composition information.

### 3.3.2 Light Scattering by Particulates: Approximations

In Section 1.1.4, we defined the size parameter,  $x = 2\pi a/\lambda$ , where  $a$  is the particle radius. Rayleigh scattering is concerned with scattering events when  $x \ll 1$ . When  $x \gtrsim 1$ , scattering events are often called *Lorenz-Mie scattering*. Lorenz (1890) and Mie (1908) independently derived the solution for the interaction of a plane wave with an isotropic homogenous sphere. The mathematical theory of Lorenz-Mie scattering begins with Maxwell's equations and will be detailed in Chapter 5, along with some new developments in research on light scattering by nonspherical ice crystals and aerosols. In this section, however, we shall present a brief discussion of Lorenz-Mie scattering and two elementary approximations: geometric optics and anomalous diffraction.

#### 3.3.2.1 LORENZ-MIE SCATTERING

The intensity scattered by a particle as a function of direction, as presented in Eq. (3.3.15), is given by

$$I(\Theta) = I_0 \Omega_{\text{eff}} \frac{P(\Theta)}{4\pi} = I_0 \left( \frac{\sigma_s}{r^2} \right) \frac{P(\Theta)}{4\pi}, \quad (3.3.23)$$

where  $I_0$  is the incident intensity,  $P$  is the phase function normalized according to Eq. (3.3.10),  $\Omega_{\text{eff}}$  is the effective solid angle upon which scattering occurs,  $r$  is the distance between the particle and the observer,  $\sigma_s$  is the scattering cross section, and  $4\pi$  is the solid angle for the entire spherical space. The scattering cross section can be derived from the Lorenz-Mie theory of light scattering by spheres and is given by the following expansion:

$$\sigma_s/\pi a^2 = Q_s = c_1 x^4 (1 + c_2 x^2 + c_3 x^4 + \dots), \quad (3.3.24)$$

where  $a$  is the radius,  $x = 2\pi a/\lambda$ ,  $Q_s$  is referred to as the *scattering efficiency*, and the coefficients in the case of nonabsorbing particles are given by

$$c_1 = \frac{8}{3} \left( \frac{m^2 - 1}{m^2 + 2} \right)^2, \quad c_2 = \frac{6}{5} \left( \frac{m^2 - 1}{m^2 + 2} \right),$$

$$c_3 = \frac{3}{175} \frac{m^6 + 41m^4 - 28m^2 + 284}{(m^2 + 2)^2} + \frac{1}{900} \left( \frac{m^2 + 2}{2m^2 + 2} \right)^2 [15 + (2m^2 + 3)^2].$$

The leading term is the dipole mode contribution associated with Rayleigh scattering. Note that for light scattering by spheres, we may replace the total number of molecules per volume  $N_s$  by  $1/V$  where  $V = 4\pi a^3/3$ . For molecules,  $a \sim 10^{-4} \mu\text{m}$ , so that  $x \sim 10^{-3}$  in the visible. Thus, the higher order terms can be neglected and the scattered intensity is proportional to  $\lambda^{-4}$ . For aerosols and cloud particles,  $a \gtrsim 10^{-1} \mu\text{m}$ , and  $x \gtrsim 1$  in the visible. In this case, the scattered intensity is less wavelength dependent and is primarily dependent on particle size. As a result, clouds and nonabsorbing aerosols in the atmosphere generally appear white. In a cloudy atmosphere, the sky appears blue diluted with white scattered light, resulting in a less pure blue sky than would have been expected from pure Rayleigh scattering.

On the basis of Eq. (3.3.23), the scattered intensity is dependent on the phase function, which can be computed from the Lorenz-Mie theory for spheres. Figure 3.13 shows typical examples of the phase function for polydispersed cloud droplets ( $\sim 10 \mu\text{m}$ ) and aerosols ( $\sim 1 \mu\text{m}$ ) illuminated by a visible light. Also shown is the phase function for Rayleigh scattering. The mean size parameters in these cases are about 100, 10, and  $10^{-3}$ , respectively. The scattering by cloud droplets is characterized by a strong forward diffraction; a minimum at  $\sim 100^\circ$  scattering angle; a peak at  $\sim 138^\circ$  scattering angle, the well-known rainbow feature; and a peak in the backscattering direction associated with the glory pattern. The diffraction pattern and the rainbow feature will be discussed further later; the explanation of the glory pattern requires more advanced discussion and will be presented in Chapter 5. The scattering of typical aerosols also displays a forward diffraction maximum and a maximum pattern in the  $150^\circ$ – $170^\circ$  scattering region (see also Fig. 1.4).

### 3.3.2.2 GEOMETRIC OPTICS

The principles of geometric optics are the asymptotic approximations of the fundamental electromagnetic theory and are valid for light-scattering computations involving a particle whose dimension is much larger than the wavelength, i.e.,  $x \gg 1$ . In this case, a light beam can be thought of as consisting of a bundle of separate parallel rays that hit the particles, which is referred to as the *localization principle*. Each ray will then undergo reflection and refraction and will pursue its own path along a straight line outside and inside the scatterer with propagation directions determined by the *Snell law*, as shown in Fig. 3.14a. In the context of geometric optics, the total electric field is assumed to consist of the diffracted rays and the reflected and refracted rays, as illustrated in Fig. 3.14b, using a sphere as an example. The diffracted rays

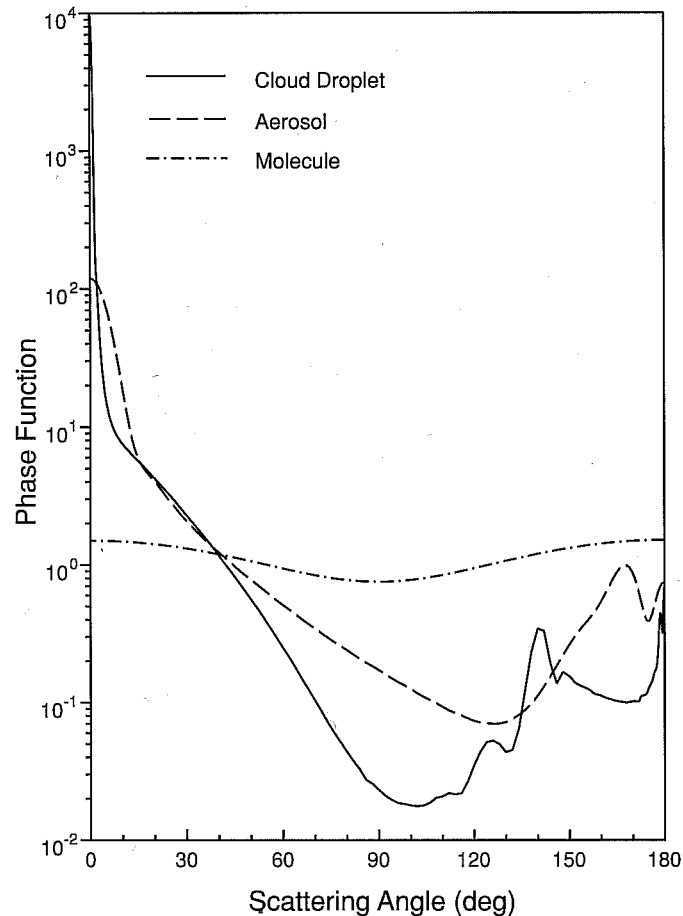


**Figure 3.13** Normalized phase functions for cloud droplets ( $\sim 10 \mu\text{m}$ ), aerosols ( $\sim 1 \mu\text{m}$ ), and molecules ( $\sim 10^{-4} \mu\text{m}$ ) illuminated by a visible wavelength of  $0.5 \mu\text{m}$ , computed from the Lorenz-Mie theory.

pass around the scatterer. The rays impinging on the scatterer undergo local reflection and refraction, referred to as *Fresnelian interaction*. The energy that is carried by the diffracted and the Fresnelian rays is assumed to be the same as the energy that is intercepted by the particle cross section projected along the incident direction.

In reference to Fig. 3.14a, let  $v_1$  and  $v_2$  be the velocities of propagation of plane waves in the two media such that  $v_1 > v_2$ . Also, let  $\theta_i$  and  $\theta_t$  be the angles corresponding to the incident and refracted waves. Thus, we have

$$\sin \theta_i / \sin \theta_t = v_1 / v_2 = m, \quad (3.3.25)$$

where  $m$  is the index of refraction for the second medium with respect to the first.

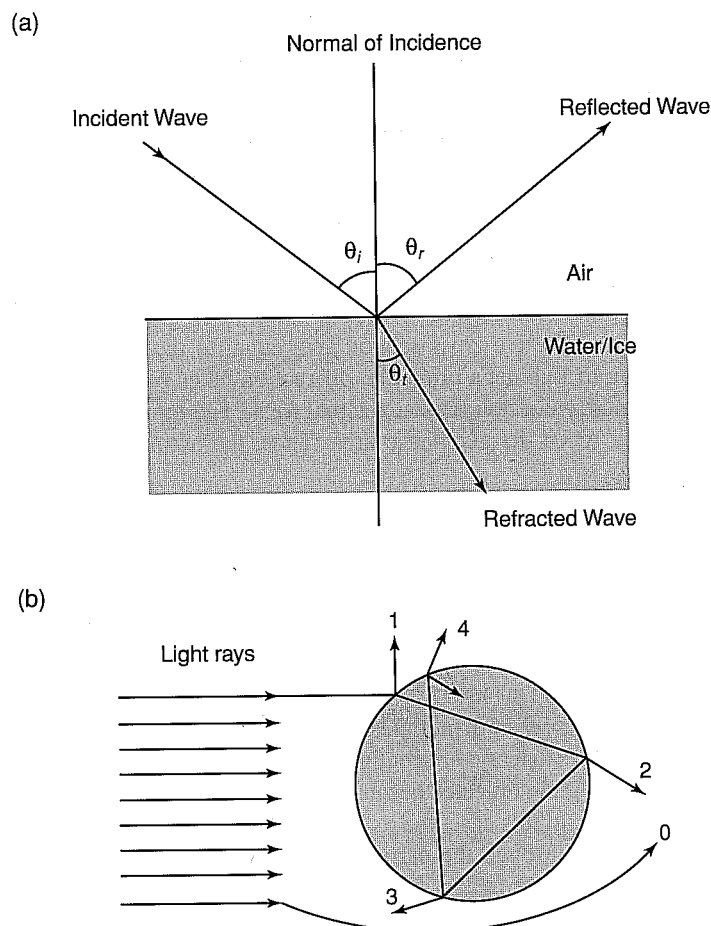


**Figure 3.14** (a) Reflection and refraction of a plane wave from air to water/ice surface. (b) Representation of light rays scattered by a sphere based on the geometric optics principle: 0, exterior diffraction; 1, external reflection; 2, two refractions; 3, one internal reflection; and 4, two internal reflections.

For the purpose of this discussion, we shall assume that there is no absorption in the medium. This is the *Snell law* relating the incident and refracted angles through the index of refraction. Exercises 3.12 and 3.13 require the derivation of the minimum deviations of light rays that produce *rainbows* from spherical water droplets and *halos* from hexagonal ice crystals. Moreover, white sunlight is decomposed into component colors after the rays undergo geometric reflection and refraction through water droplets and ice crystals.

The diffraction component in geometric optics can be determined from *Babinet's principle*. This principle states that the diffraction pattern in the far field, referred to as *Fraunhofer diffraction*, from a circular aperture is the same as that from an opaque

disk or sphere of the same radius. Based on this principle and geometric consideration, the scattered intensity is proportional to

$$I_p = \frac{x^4}{4} \left[ \frac{2J_1(x \sin \Theta)}{x \sin \Theta} \right]^2, \quad (3.3.26)$$

where  $J_1$  is the first-order *Bessel function* and  $\Theta$  is the scattering angle. Exercise 3.14 requires the calculation of maxima and minima of the diffraction pattern that can be used to explain an optical phenomenon known as the *corona*.

One final note is in order here. If a particle of any shape is much larger than the incident wavelength, the total energy removed is based on geometric reflection and refraction, giving an effective cross-section area equal to the geometric area  $A$ . In addition, according to Babinet's principle, diffraction takes place through a hole in this area, giving a cross-section area also equal to  $A$ . The total removal of incident energy is therefore twice the geometric area. Thus, the extinction cross section is given by

$$\sigma_e = 2A, \text{ or } Q_e = \sigma_e/A = 2, \quad (3.3.27)$$

where  $Q_e$  is called the *extinction efficiency*. This is referred to as the *optical theorem of extinction*. If a particle is nonabsorbing, then we have  $Q_e = Q_s$ , where the extinction and scattering efficiencies are the same.

### 3.3.2.3 ANOMALOUS DIFFRACTION THEORY

Consider large optically soft particles such that  $x \gg 1$  and  $|m - 1| \ll 1$ . The second condition implies that rays are negligibly deviated as they cross the soft particle boundary and are negligibly reflected because the refractive indices inside and outside the particle are similar. In this case, the extinction is largely caused by absorption of the light beam passing through the particle, as well as by the interference of light passing through the particle and passing around the particle. This is the physical foundation for the anomalous diffraction theory originally developed by van de Hulst (1957). In reference to Fig. 3.15, let the plane wave be incident on a spherical particle with a radius  $a$  and a refractive index  $m \rightarrow 1$ . The wave front on the forward side of the particle can be divided into two types: one within the geometric shadow area denoted by  $A = \pi a^2$ , and one outside this area denoted by  $B$ . The incident rays can undergo diffraction and pass around the particle. The rays can also hit the particle and undergo reflection and refraction. Since  $m \rightarrow 1$ , we may assume that the rays enter into the particle and pass through it, as illustrated in Fig. 3.15. However, these rays will have phase lags due to the presence of the particle. The phase lag for the ray indicated in the figure is  $2a \sin \alpha (m - 1) \cdot 2\pi/\lambda$ . If we define the phase shift parameter

$$\rho = 2x(m - 1), \quad (3.3.28)$$

the phase lag can then be expressed by  $\rho \sin \alpha$ .

Consider a screen that collects the field. The resultant wave on the screen is the sum of the incident and scattered fields. If the incident field is assumed to be unity,

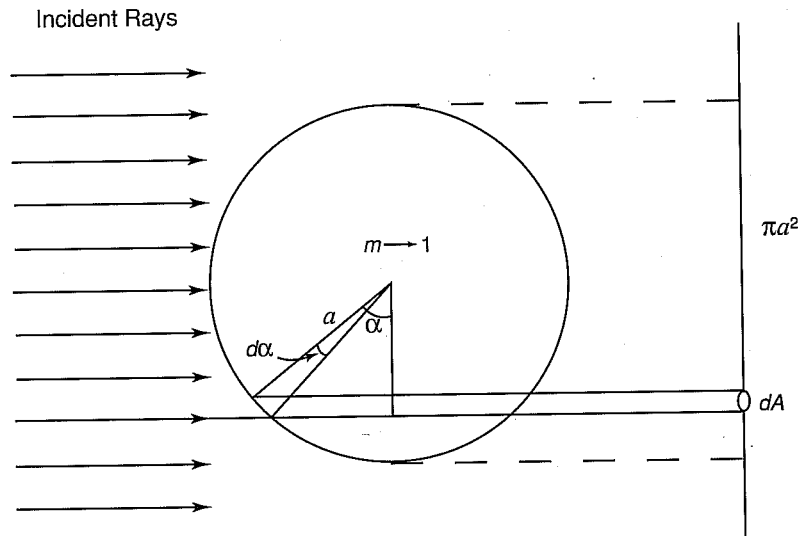


**Figure 3.15** Geometry of anomalous diffraction through a sphere with a radius  $a$  and an index of refraction  $m \rightarrow 1$ .  $\pi a^2$  denotes the geometric cross-section area of the sphere and  $dA$  denotes the differential cross-section area.

then in the forward direction ( $\Theta = 0$ ), the change in the electric field is proportional to

$$A = \iint (1 - e^{-i\rho \sin \alpha}) dx dy. \quad (3.3.29a)$$

The differential area can be replaced by an area in the polar coordinate such that  $dx dy = a \cos \alpha d(a \cos \alpha) d\phi$ . Thus, we have

$$A = \int_0^{2\pi} \int_0^{\pi/2} (1 - e^{-i\rho \sin \alpha}) a^2 \sin \alpha d \sin \alpha d\phi = 2\pi a^2 K(i\rho), \quad (3.3.29b)$$

where

$$K(i\rho) = \frac{1}{2} + \frac{e^{-i\rho}}{i\rho} + \frac{e^{-i\rho} - 1}{(i\rho)^2}. \quad (3.3.30)$$

The extinction cross section  $\sigma_e$  is proportional to the differential change in the scattered intensity  $I$ . Since  $I \sim |E|^2$ , as shown in Eq. (3.3.6),  $dI \sim 2d|E|$ . Thus, we have  $\sigma_e = 2\text{Re}(A)$ . It follows that the extinction efficiency is given by

$$Q_e = \sigma_e / \pi a^2 = 4\text{Re}[K(i\rho)] = 2 - \frac{4}{\rho} \sin \rho + \frac{4}{\rho^2} (1 - \cos \rho), \quad (3.3.31)$$

where  $\text{Re}$  denotes the real part of the function. Exercise 3.15 requires calculations of  $Q_e$ .

We may also determine the absorption efficiency by the following procedure. The ray path as shown in Fig. 3.15 is  $l = 2a \sin \alpha$ . The absorption coefficient  $k_i = m_i 2\pi / \lambda$ ,

where  $m_i$  is the imaginary part of the refractive index. Thus, the absorption path length associated with the electric field is  $lk_i$ . The attenuation of the intensity of the ray is then  $\exp(-2lk_i)$  and the absorption cross section for all possible rays is

$$\sigma_a = \int \int (1 - e^{-2lk_i}) dx dy. \quad (3.3.32)$$

Following the procedure just illustrated, the absorption efficiency is given by

$$Q_a = \sigma_a/\pi a^2 = 1 + \frac{2}{b}e^{-b} + \frac{2}{b^2}(e^{-b} - 1), \quad (3.3.33)$$

where  $b = 4xm_i$  and  $x = 2\pi a/\lambda$ . The approximation based on the anomalous diffraction theory (ADT) is useful for the calculation of the extinction and absorption coefficients when  $m \rightarrow 1$ . It can also be applied to nonspherical particles such as spheroids and hexagons. Since refractions and reflections of rays are neglected in this approximation, its accuracy must be examined carefully when applied to the scattering of ice crystals ( $m \sim 1.31$ ) and aerosols ( $m \sim 1.5$ ). Finally, it should be noted that the ADT approximation cannot produce the phase function pattern.

### 3.4 Multiple Scattering and Absorption in Planetary Atmospheres

#### 3.4.1 Fundamentals of Radiative Transfer

In Section 1.1.4, we pointed out that scattering is often coupled with absorption. In the following we formulate the fundamental equation governing the transfer of diffuse solar radiation in plane-parallel atmospheres. The term *diffuse* is associated with multiple scattering processes and is differentiated from *direct* solar radiation. In reference to Fig. 3.16 and considering a differential thickness  $\Delta z$ , the differential change of diffuse intensity emergent from below the layer is due to the following processes: (1) reduction from the extinction attenuation; (2) increase from the single scattering of the unscattered direct solar flux from the direction  $(-\mu_0, \phi_0)$  to  $(\mu, \phi)$ ; (3) increase from multiple scattering of the diffuse intensity from directions  $(\mu', \phi')$  to  $(\mu, \phi)$ ; and (4) increase from emission within the layer in the direction  $(\mu, \phi)$ . Consider a small volume containing a spectrum of molecules and/or particulates and denote the extinction, scattering, and absorption coefficients (in units of per length) as  $\beta_e$ ,  $\beta_s$ , and  $\beta_a$ , respectively, defined by

$$\beta_{e,s,a} = \int_{\Delta z} \sigma_{e,s,a}(z)n(z) dz/\Delta z, \quad (3.4.1)$$

where the symbol  $\sigma$  denotes the cross section and  $n$  is the number density. Moreover, let the phase function corresponding to a volume of particulates be  $P$ . Thus,  $P(\mu, \phi; \mu', \phi')$  denotes the redirection of the incoming intensity defined by  $(\mu', \phi')$  to the outgoing intensity defined by  $(\mu, \phi)$ . Also note that the differential length